Neurotoxicology 74 (2019) 221–229

Contents lists available at ScienceDirect

Neurotoxicology

journal homepage: www.elsevier.com/locate/neuro

Full Length Article

Triclosan induces PC12 cells injury is accompanied by inhibition of AKT/mTOR and activation of p38 pathway

Shao-Jun Li[a], Pan Chen[b], Tanara Vieira Peres[d], Beatriz Ferrer Villahoz[b], Ziyan Zhang[b], Mahfuzur R. Miah[b,c], Michael Aschner[b,c,*]

[a] Department of Toxicology, School of Public Health, Guangxi Medical University, Nanning 530021, China
[b] Department of Molecular Pharmacology, Albert Einstein College of Medicine, Bronx, NY10461,United States
[c] Department of Neuroscience, Albert Einstein College of Medicine, Bronx, NY 10461, United States
[d] Department of Biochemistry, Federal University of Santa Catarina, Florianopolis, SC, 88040900, Brazil

ARTICLE INFO

Keywords:
Triclosan
Apoptosis
PC12
AKT/mTOR pathway
p38

ABSTRACT

Triclosan (TCS) has been widely used as a disinfectant and antiseptic in multiple consumer and healthcare products due to its clinical effectiveness against various bacteria, fungi and protozoa. Recently, several studies have reported the adverse effects of TCS on various nerve cells, arousing concerns about its potential neurotoxicity. The present study aimed to investigate the neurotoxicity of TCS in rat pheochromocytoma PC12 cells. After differentiation, the stabilized PC12 cells were treated with 1, 10, 50 μM TCS for 12 h. At the end of the treatment, the generation of reactive oxygen species (ROS), protein expression of apoptotic-related genes, AMPK-AKT/mTOR, as well as p38 in PC12 cells were determined. The concentrations were chosen based on the results of cell viability and lactic dehydrogenase (LDH) assays in response to TCS treatment (ranging from 0.001 to 100 μM) for varied time periods. The results showed that TCS is cytotoxic to PC12 cells, causing decreased cell viability accompanied by increased LDH release. TCS treatment at 10 and 50 μM for 12 h increased the mRNA and protein expression of the pro-apoptotic gene Bax, while Bcl-2 levels remained unchanged. Moreover, an increase in the generation of reactive oxygen species (ROS) was found in TCS-treated PC12 cells at the concentrations of 1 and 10 μM. Pretreatment with 100 μM N-acetyl cysteine (NAC- ROS scavenger) for 1 h normalized the ROS generations in TCS-treated PC12 cells. Additionally, the suppression of the phosphorylation of Akt and mTOR was observed in TCS-treated PC12 cells at 10 and 50 μM for 12 h, concomitant with the activation of p38 MAPK pathway at 50 μM TCS. However, there were no effects of TCS on the phosphorylation of AMPK in these cells. Taken together, these results suggest that TCS may cause adverse effects and oxidative stress in PC12 cells accompanied by inhibition of Akt/mTOR and activation of p38.

1. Introduction

Triclosan (TCS), a broad-spectrum antibacterial agent, has been widely used in numerous consumer products since the 1960s, including personal care, skin-care products, sanitizing products, house hold items etc (Rodricks et al., 2010; Koeppe et al., 2013; Liu et al., 2016). Singer et al (Singer et al., 2002) estimated the quantity of TCS used reached approximately 1500 tons/ year in consumer products in the United States alone. Recently, several studies reported detectable levels of TCS or its metabolites in drinking water, biosolids and aquatic sediments (Yu et al., 2011; Bedoux et al., 2012; Zhou et al., 2017; Zhang et al., 2019). It is estimated that over 110 tons/ year of TCS are annually discharged into the water in the United States alone (Heidler and Halden, 2007). Although the added dosage of TCS is limited only up to 0.3% in the daily necessities, the Scientific Committee on Consumer Safety stressed that repeated exposure to TCS from various TCS-containing products over time might pose a risk to humans (SCCS, 2010).Recently, several studies reported on the presence of TCS in the brain (13–88 ng/g wet weight) and liver (110–910 ng/g wet weight) of fish (Tanoue et al., 2014), as well as in other aquatic organisms. Some studies have suggested that TCS is metabolized and eliminated from the human body, without accumulation or its detection in organs (Bagley and Lin, 2000). However, subsequently a large number of studies have shown the presence of TCS in various human organs and body fluid, such as adipose tissue liver (mean 0.44 ng/g) (Wang et al., 2015), brain (0.23 ng/g) (Geens et al., 2012), breast milk (0.019-2.1 ng/g lipid)

* Corresponding author at: Department of Molecular Pharmacology, Albert Einstein College of Medicine, Bronx, NY, 10461, United States.
E-mail address: Michael.Aschner@einstein.yu.edu (M. Aschner).

https://doi.org/10.1016/j.neuro.2019.07.008
Received 23 May 2019; Received in revised form 18 July 2019; Accepted 29 July 2019
Available online 02 August 2019
0161-813X/

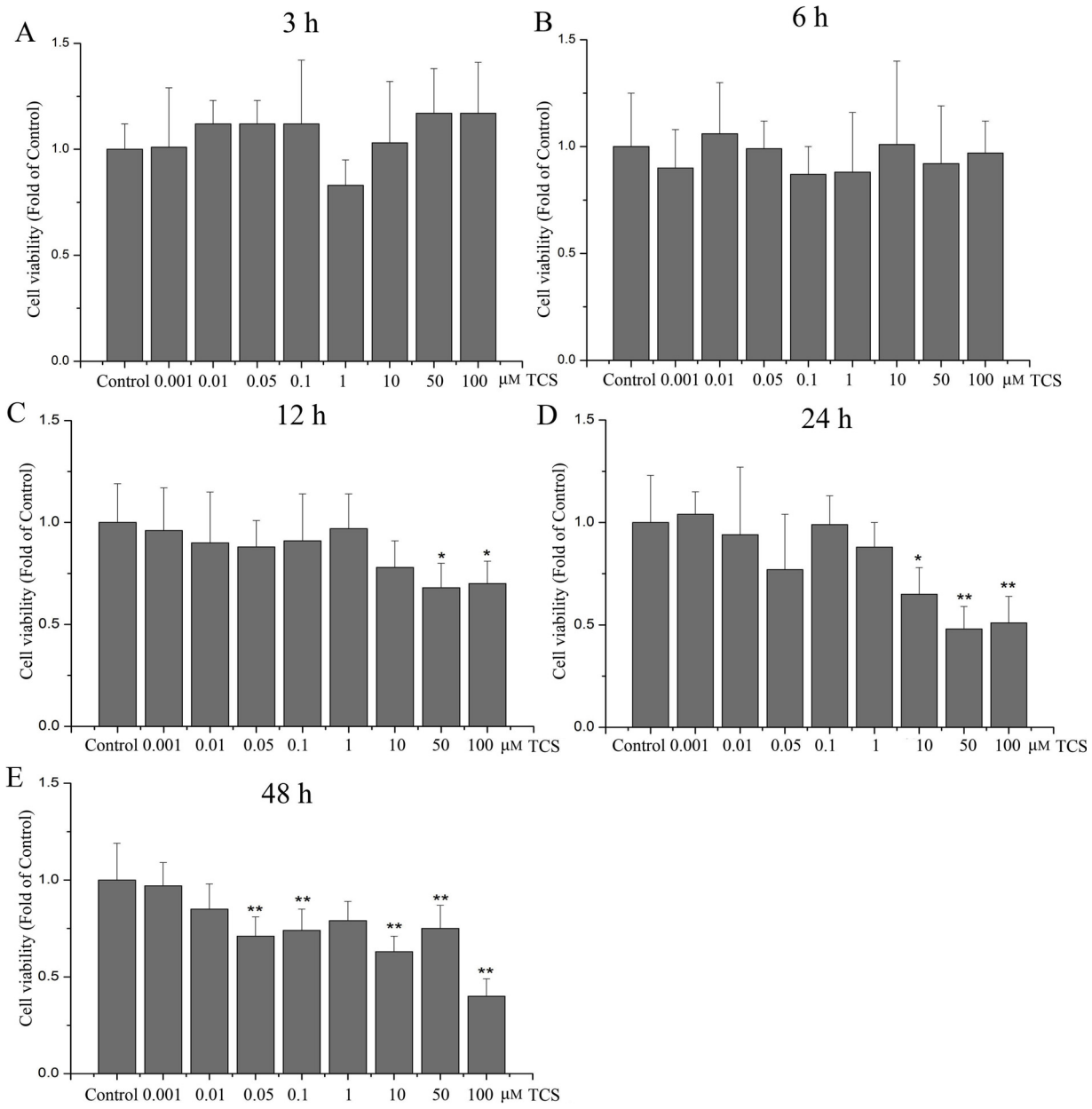

Fig. 1. TCS effect on cell viability in PC12 cells.
Cell viability was determined by MTT at different doses and time points of TCS treatment in PC12 cells. Treatment with 0.001–100 μM TCS for (A) 3 h; (B) 6 h; (C) 12 h; (D) 24 h; (E) 48 h. Data were expressed as the fold of cell viability relative to the Control. $^{*}p < 0.05$ or $^{**}p < 0.01$ vs. Control. N = 6.

(Allmyr et al., 2006; Dayan, 2007), serum (0.52–354 ng/L) (Allmyr et al., 2008; Dirtu et al., 2008), plasma (0.01–38 ng/g) (Allmyr et al., 2006), urine(Kalloo et al., 2018; Dix-Cooper and Kosatsky, 2019; Juric et al., 2019), and cord blood (0.1–1.3 ng/g serum) (Pycke et al., 2014) etc., indicating accumulation of TCS, potentially even at higher levels than previously estimated (Mustafa et al., 2003). Collectively, these studies suggest that the widespread use of TCS.

It is noteworthy that an epidemiologic study noted a close relationship between elevated TCS levels in urine at birth and lower cognitive test scores of children (Jackson-Browne et al., 2018), suggesting a potential toxicity of TCS to the central nervous system (CNS). While the mechanisms of its neurotoxicity have yet to be delineated. A series of studies reported that TCS has several adverse effects on cardiac and skeletal muscle by interrupting Ca^{2+} signaling (Cherednichenko et al., 2012; Yueh et al., 2014; Yan et al., 2019). Earlier studies reported that TCS activated the Fasdependent apoptosis in the primary cultured cortical neurons (Szychowski et al., 2015). Subsequently, Park et al showed that TCS induced apoptosis by increasing the generations of reactive oxygen species (ROS) (Park et al., 2016). Other studies have demonstrated that TCS at environmentally relevant levels induced apoptosis accompanied by inhibition of N-methyl-D-asparagic acid receptor (NMDAR) subunits and Ca2+ transient in primary cultured neocortical or hippocampal neurons(Arias-Cavieres et al., 2018; Szychowski et al., 2019).

MAPKs plays critical roles in regulating normal cell functions, including apoptosis, oxidative stress and differetiation. Interestingly, both *in vitro* and *in vivo* studies showed that TCS treatment induced activation of the p38 pathway (Zhang et al., 2018). In addition, other signaling pathways, such as mammalian target of rapamycin (mTOR), Akt and AMP activated protein kinase (AMPK) have been shown to be involved in the adverse effects of TCS on non-nerve cells (Cao et al., 2017; Wang et al., 2018a,b,c). Whether these latter pathways are involved in TCS-induced neurotoxicity has yet to be determined.

PC12 cells, a commonly used neuronal cell model, is derived from a

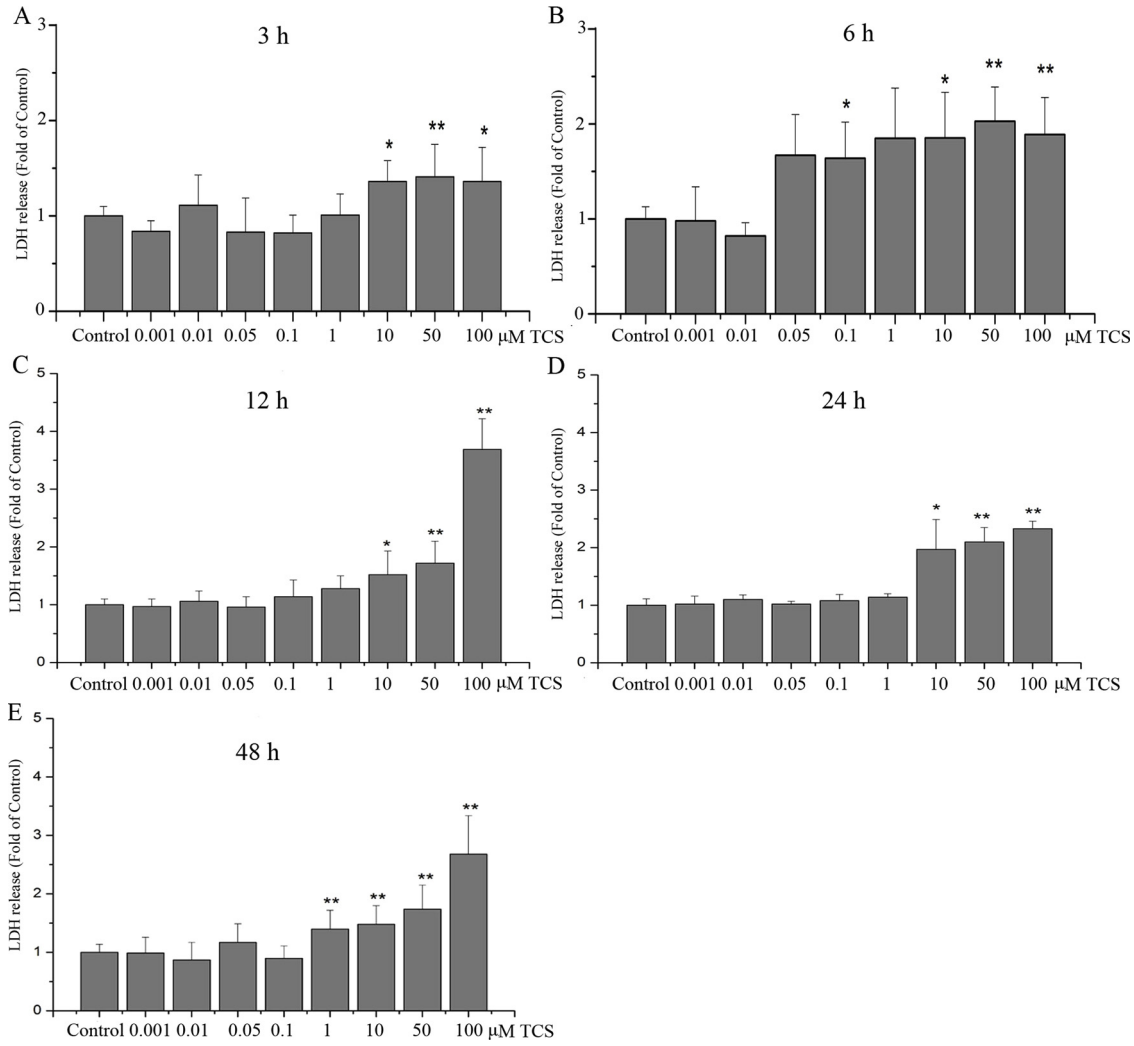

Fig. 2. TCS effect on LDH release in PC12 cells.
Integrity of cell membrane was determined at different doses and time points of TCS treatment in PC12 cells with the LDH assay. Treatment with 0.001–100 μM TCS for (A) 3 h; (B)6 h; (C)12 h; (D) 24 h; (E) 48 h. Data were expressed as the fold of LDH release relative to the Control. $^{*}p < 0.05$ or $^{**}p < 0.01$ vs. Control. N = 6.

transplanted pheochromocytoma of rat and was described by Greene and Tischler (Greene and Tischler, 1976). These cells have been widely used as a valuable model to evaluate the effects of environmental agents on the dopaminergic system, neuronal development and neurodegenerative diseases (Zhao et al., 2017; Benseny-Cases et al., 2018). To our knowledge, however, information is not available on the effects of TCS on PC12 cells. The present study aimed to 1) investigate the effects of TCS on injuries in PC12 cells by determining the cell viability, membrane integrity and apoptotic-related genes expression, and 2) explore the mechanisms of TCS-induced neurotoxicity by determining redox status changes and protein expressions of AMPK-AKT/mTOR as well as p38 in PC12 cells.

2. Materials and methods

2.1. PC12 cells culture and treatment

Rat pheochromocytoma PC12 cells were cultured in medium containing 5% heat-inactivated fetal bovine serum (FBS), 10% horse serum (Gibco, Grand Island, NY, USA), 100 IU/mL penicillin, and 100 μg/mL streptomycin antibiotic-free RPMI 1640 medium. Cells were cultured in an incubator containing 5% CO_2 at 37 °C with stable humidity. The culture medium was replaced twice a week. To obtain neuron-like PC12 cells, cells were maintained with differentiating medium (containing RPMI1640 medium with 10% FBS, 5% horse serum and 25 ng/mL of nerve growth factor). The cells were cultured with nerve growth factor every other day with differentiating medium until ready for experiment.

The differentiated PC12 cells were randomly divided into four groups: Solvent Control (Control), 1, 10 or 50 μmol/L (μM) TCS groups. In the Control, 1, 10 or 50 μM TCS groups, the cells were treated with 0, 1, 10 or 50 μM TCS (Sigma-Aldrich) for 12 h (hr), respectively. The concentrations of TCS were selected according to the results of cell viability via treating with 0, 0.001, 0.01, 0.05, 0.1, 1, 10, 50 or 100 μM TCS for 3, 6, 12, 24 and 48 h.

2.2. Cell viability

Briefly, cells were seeded in 96-well plates, which were precoated with Poly-D-Lysine with a density of 2×10^4 cells/well. At the designated time points, cell viability was detected by MTTassay. After removal of the medium, a total of 20 μL 3-(4,5-dimethylthiazol-2-yl)-2,5-diphenyltetrazolium bromide (MTT) solutions (5 mg/ml) and 100 μL of medium were added to each well and incubated in the incubator for 4 h. 150 μL dimethylsulfoxide was added to each well to dissolve the formazan after discarding the supernatant. The absorbance values were quantified by using a spectrophotometer (Molecular Devices, VMax Kinetic Microplate Reader, and Sunnyvale, CA) at a wavelength of

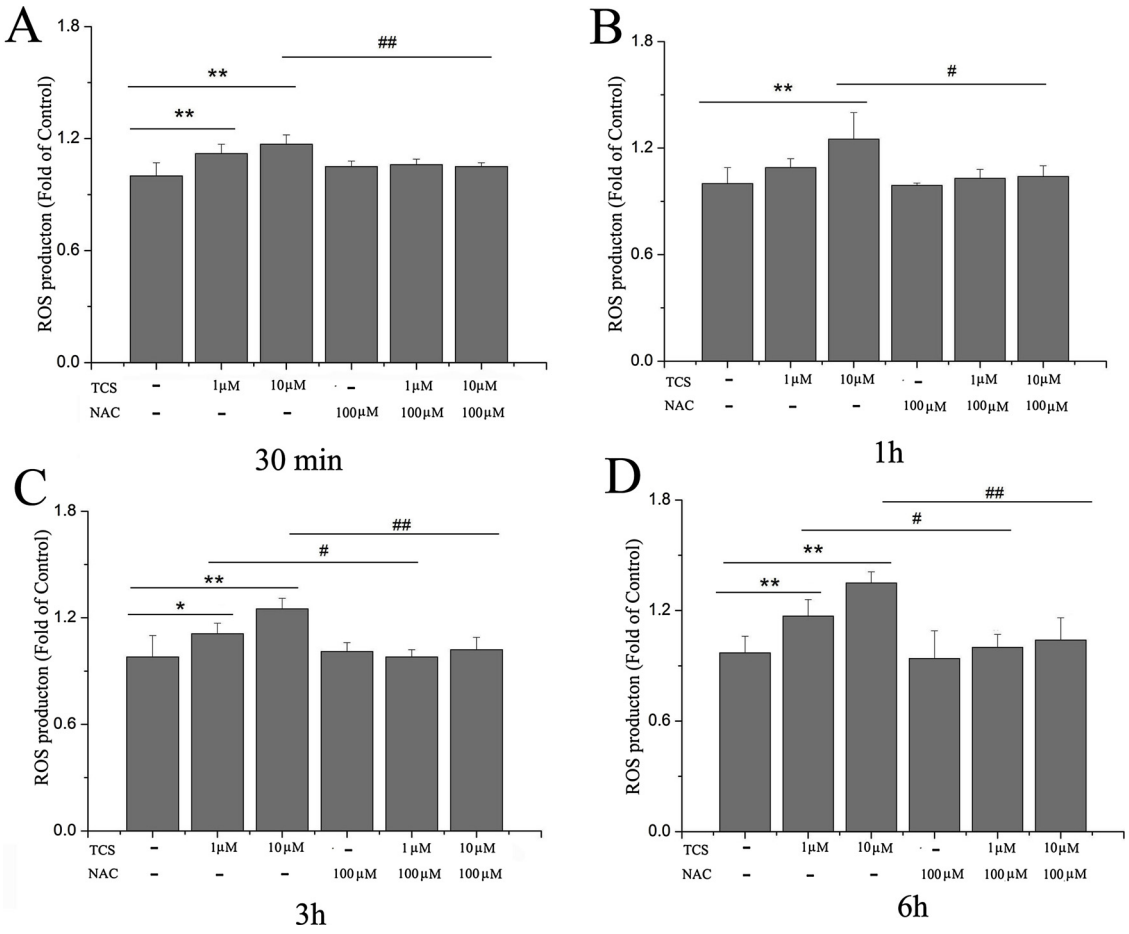

Fig. 3. TCS effect on ROS in PC12 cells.
ROS releases in PC12 cells were determined from different doses and time points of TCS treatment with DCFH-DA. Cells were treated with 1 and 10 μM TCS subsequent to pretreatment with 100 μM NAC for 1 h. TCS treatment for (A) 30 min; (B) 1 h; (C) 3 h; (D) 6 h. Data were expressed as the fold of ROS generation relative to Control. $^{*}p < 0.05$ or $^{**}p < 0.01$ vs. Control; $^{\#}p < 0.05$ or $^{\#\#}p < 0.01$ vs. the TCS treatment group at the same time point. N = 6.

490 nm. The data was expressed as a percentage of the Control.

2.3. Assay of lactate dehydrogenase (LDH)

Cell membrane integrity was evaluated by using a LDH cytotoxicity detection kit, following manufacturing instructions. Briefly, after treatment, 100 μL of culture supernatant from each well was collected and transferred to a new 96-well plate. Then 50 μL of reaction mixture from the LDH cytotoxicity detection kits, were added to each well. Subsequently, the plate was incubated at room temperature in dark. The reaction was stopped after 30 min reaction by adding 50 μL of stopping solution, provided from the detection kit to each well. The absorbance was detected with a spectrophotometer at a wavelength of 490/690 nm.

2.4. Determination of intracellular ROS

The ROS scavenger N-acetyl cysteine (NAC) was used to confirm the effects of TCS on ROS generations in PC12 cells. PC12 cells were pretreated with100 μM NAC for 1 h followed by treatment with 1 and 10 μM TCS for 30 min, 1, 3 and 6 h. At the designated time points, changes in intracellular ROS were measured by using 2′,7′-Dichlorodihydrofluorescein diacetate(DCFH-DA, Beyotime Institute of Biotechnology). Here, we selected 30 min, 1, 3 and 6 h to study the ROS generation induced by TCS treatment. At the end of the treatment, the medium was removed and washed three times with PBS; then, 100 μL serum-free culture medium containing 10 μM DCFH-DA was added to each well. After incubation for 30 min in dark at 37 °C, cells were washed with PBS in triplicate. Subsequently, 100 μL fresh RPMI 1640 medium (without FBS and horse serum) was added to each well. The fluorescence intensities were recorded with a spectrophotometer with an excitation of 485 nm and an emission of 535 nm.

2.5. RNA extraction and real-time quantitative PCR (RT-qPCR)

According to the manufacturer's instructions, the total RNA was isolated from cultured cells by using Trizol Reagent. The levels and purity of RNA samples were detected through NanoDrop 2000 Spectrophotometer (Thermo Scientific, San Jose, CA, USA). Subsequently, the purified RNA samples were reversely transcribed into cDNA by using cDNA Reverse Transcription kits (Thermo Scientific, San Jose, CA, USA).

Lastly, the cDNA was used to perform RT-qPCR by using a thermocycler CFX96 Real-time system with BioRad CFX manager software (BioRad, Hercules, CA, USA) according to the manufacturer's protocol. All reactions were performed in triplicate. The relative quantifications of each target gene was carried out by using the $2^{-\Delta\Delta}$Ct method and then normalized to the control samples. For RT-qPCR, the following specific TaqMan probes which were bought from Applied Biosystems Gene of interest/Assay ID were used for each gene: Bax rat/ Rn01480160_g1; Bcl-2 rat/ Rn99999125_m1; GAPDH rat/ Rn01775763_g1.

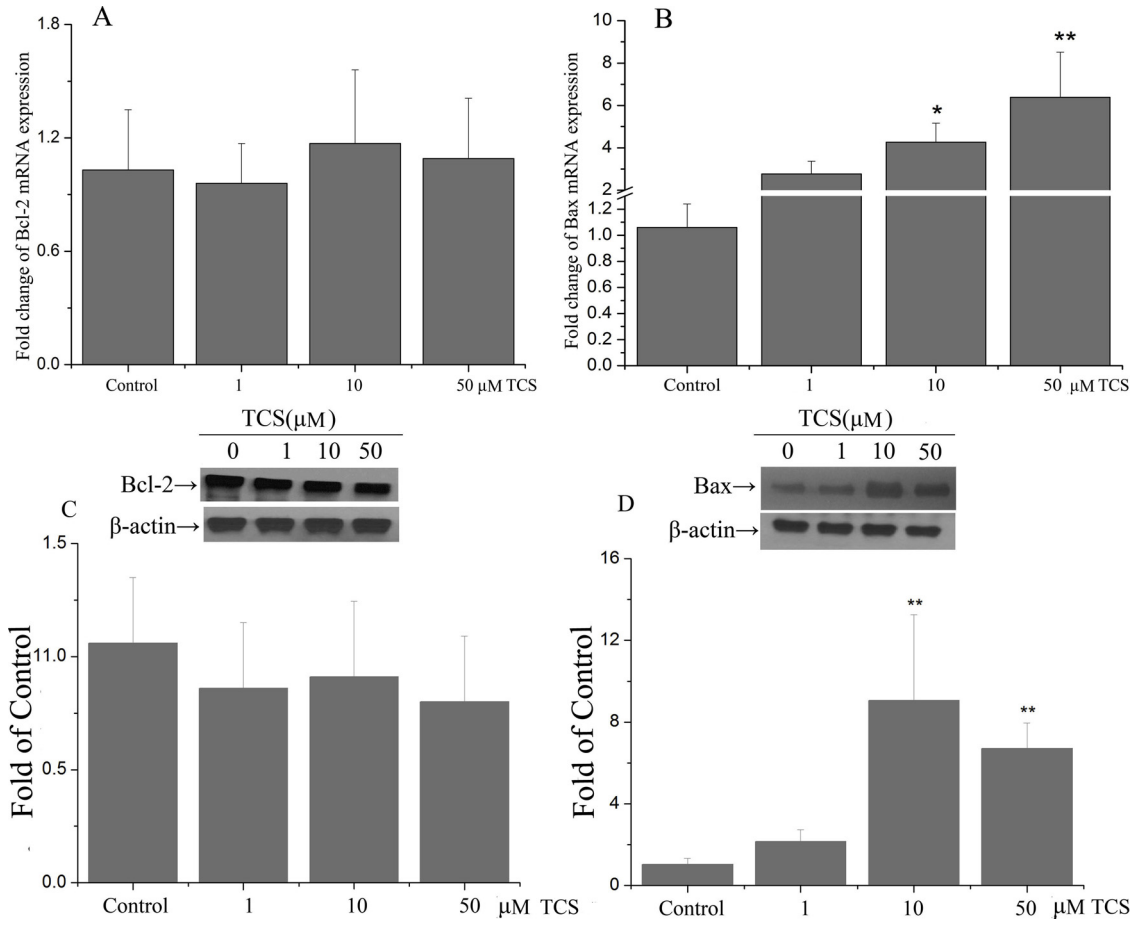

Fig. 4. TCS effect on mRNA and protein expressions of apoptosis-related proteins in PC12 cells.
The mRNA and protein expressions of apoptosis-related genes (including Bax and Bcl-2) were assessed in PC12 cells after treated with 1, 10, 50 μM TCS for 12 h by using RT-qPCR and western blotting. Changes in mRNA expressions of Bcl-2 (A) and Bax (B) and Changes in protein expression of Bcl-2(C) and Bax (D) were measured. Band intensities were quantified with Image-Pro Plus 6.0. The protein expression of Bax and Bcl-2 were normalized to β-actin. Data were expressed as the fold of mRNA or protein expression of target genes relative to the Control. $^{*}p < 0.05$ or $^{**}p < 0.01$ vs. Control. N = 5.

2.6. Western blotting analysis

After treatments, the cells samples were collected and washed twice with PBS. Then proteins from cells were extracted with ice-cold RIPA lysis buffer that contains 1% protease inhibitor, and phosphatase inhibitor cocktail 2 (Sigma) and 3 (Sigma) was added. Protein concentrations of all samples were measured by using the BCA kits (Thermo Fisher). Twenty micrograms of total protein were separated by gel electrophoresis (SDS-PAGE), and then transferred to nitrocellulose membranes. After blocking with 5% bovine serum albumin (BSA) in tris buffered saline (TBS) at room temperature for 1 h, the membranes were incubated with primary antibody overnight at 4 °C. All concentrations of each antibody were listed as follow (v: v): phospho AMPK (Cell signaling, 1:1000), total/ phospho p38 (Cell signaling, 1:1000), Bax (Santa Cruz, 1:1000), Bcl-2 (Santa Cruz, 1:1000), total/phospho mTOR (Cell signaling, 1:1000) or β-actin (Sigma, 1:10,000). Subsequently, the membranes were incubated with HRP conjugate secondary antibodies against mouse (Invitrogen, 1:10,000), goat (Thermo Scientific, 1:10,000), or rabbit (Thermo Scientific, 1:10,000) in TBS-T (TBS containing 0.1% Tween-20, pH = 7.5) containing 5% BSA at room temperature for 1 h. All steps were followed by 5 min washes with TBS-T in triplicate. Finally, membranes were developed with chemiluminescent reaction. Lastly, the bands were quantified using ImageJ (National Institutes of Health, Bethesda, MD, USA, http://imagej.nih. gov/ij/). Protein expression levels were standardized by β-actin in different cell substrates.

2.7. Statistical analysis

All statistical analyses were performed by using SPSS 16.0 for Windows (SPSS, Inc, Chicago, USA). To compare the means among the groups, One-way analysis of variance (ANOVA) was adopted. Subsequently, the *post hoc* Tukey's test was performed to account multiple comparisons. Significance was set at $p < 0.05$. Data were expressed as the standard error of the mean (mean ± S.E.M).

3. Results

3.1. Effects of TCS on cell viability in PC12 cells

Cell viability in PC12 cells was determined with the MTT assay upon 0.001–100 μM TCS treatment for 3, 6, 12, 24 and 48 h. TCS exposure to 0.001–100 μM for 3 and 6 h had no significant effects on cell viability ($p > 0.05$, Fig.1 A and B). Upon exposure to 50–100 μM TCS for 12 h, cell viability was decreased ($p < 0.05$, Fig.1 C). After 24 h exposure to 10, 50 or 100 μM TCS, cell viability was decreased to 65%, 51% and 48%, respectively ($p < 0.05$ or 0.01, Fig.1 D). At the 48 h time point, TCS treatment up to 0.05 μM significantly reduced PC12 cells viability ($p < 0.05$ or 0.01, Fig.1 E).

3.2. Effects of TCS on LDH release from PC12 cells

To determine the effects of TCS on the integrity of PC12 cells

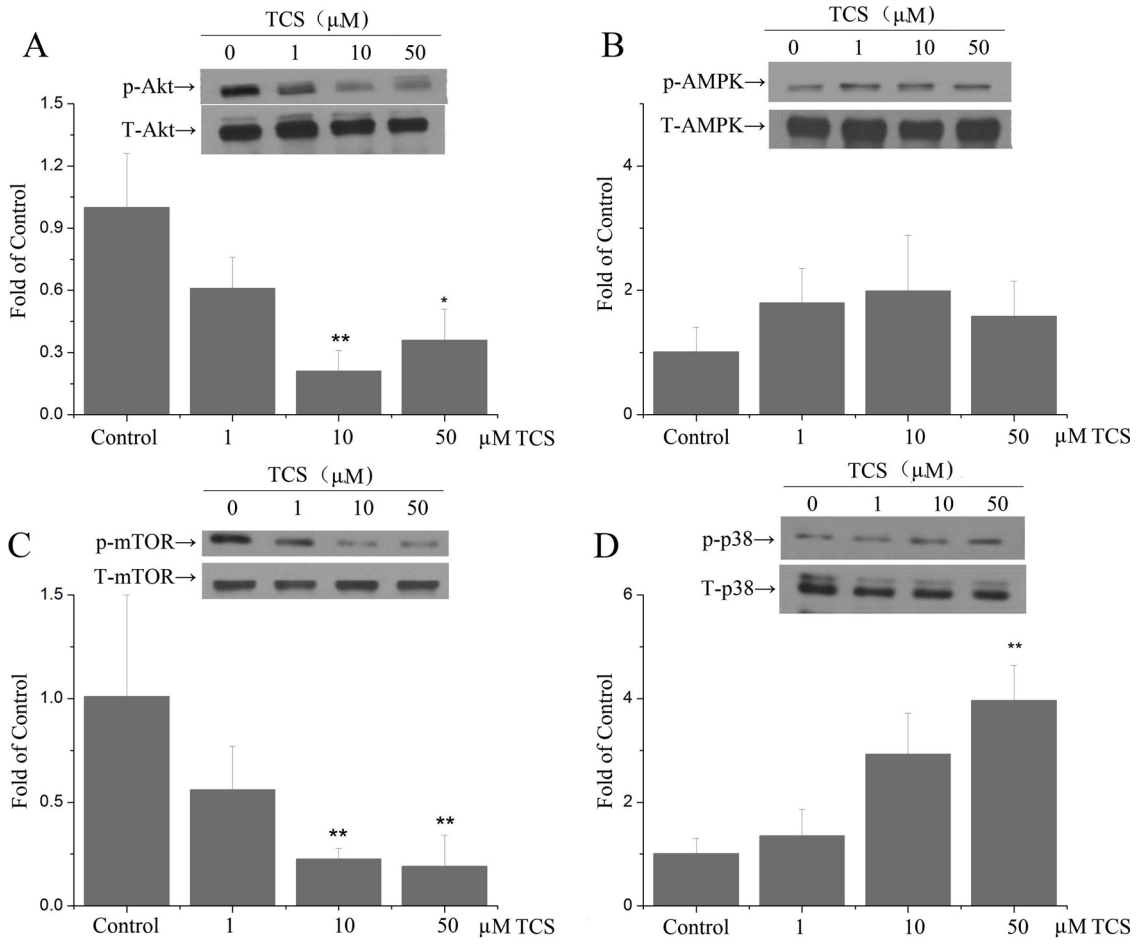

Fig. 5. Effects of TCS on AMPK/Akt in PC12 cells.
PC12 cells upon 1, 10 and 50 μM TCS treatment for 12 h. Phosphorylation of (A) Akt; (B) AMPK; (C) mTOR; (D) p38 in PC12 cells. p-Akt, p-mTOR and p-p38 levels were normalized to total Akt, mTOR or p38, respectively. Phosphorylation of AMPK was normalized to β-actin. Western blotting was analyzed with Image-Pro Plus 6.0.Data was expressed as the fold of the protein expression of target proteins relative to the Control. $^{*}p < 0.05$ or $^{**}p < 0.01$ vs. Control. N = 5.

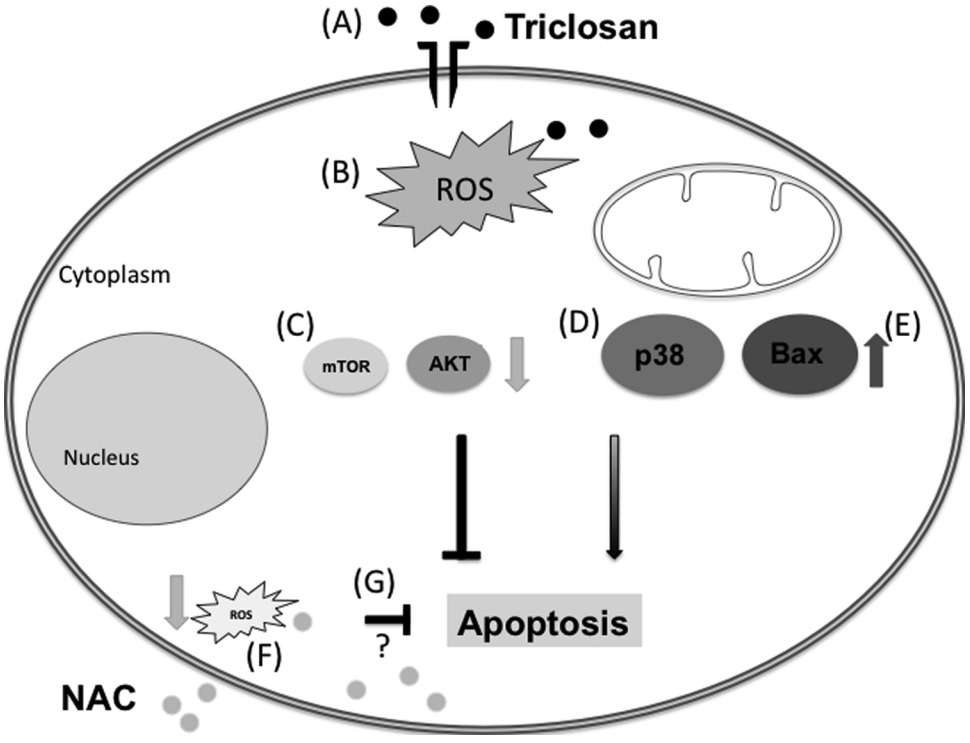

Fig. 6. Signaling pathways altered by TCS exposure.
Upon exposure to 50 μM TCS for 12 h, PC12 cells viability was decreased (A), and ROS production was increased (B). Both anti-apoptotic proteins mTOR and Akt (C) display decreased phosphorylation. We also observed increased phosphorylation of p38 MAPK (D), which has been shown to participate in apoptosis. Due to increased expression of Bax (E), it is likely that apoptosis takes place. Treatment with N-acetyl cysteine (NAC) decreased ROS in this model (F). However it remains to be determined whether oxidative stress plays a role in the alterations observed in this study (G).

membrane, LDH release was measured. At almost all tested time periods (3–24 hr), LDH release in PC12 cells was not affected by treatment with a dose lower than 1 μM TCS ($p > 0.05$, Fig.2). While treated with 1–100 μM TCS for a longer period (48 h) increased LDH release in PC12 cells. In addition, it induced a concentration-dependent increase in LDH release at 10, 50 and 100 μM, at all time periods ($p < 0.05$ or 0.01, Fig.2). Interestingly, treatment with 100 μM TCS for 3–12 hr induced increased LDH release in a time-dependent manner ($p < 0.05$ or 0.01, Fig.2A, B and C).

3.3. TCS treatment increased ROS generation in PC12 cells

Both TCS treatment at 1 and 10 μM increased ROS generation in PC12 ($p < 0.05$ or 0.01, Fig.3), with the exception of the 1 h time point ($p > 0.05$, Fig.3 B). Pretreatment with a ROS scavenger, NAC, reduced the ROS generation in response to TCS treatment ($p < 0.05$ or 0.01, Fig.3). Treatment with NAC alone had no effects on ROS generation ($p > 0.05$, Fig.3).

3.4. TCS treatment increased mRNA and protein expression of Bax, but had no effect on Bcl-2 in PC12 cells

Based on the MTT and LDH studies, we selected 1, 10 and 50 μM for further evaluation of the effects of TCS on PC12 cells. Pro- or anti-apoptotic proteins play critical roles in the regulation of cellular apoptosis, particularly Bax and Bcl-2. The present study assessed the mRNA and protein expression of these two genes. TCS treatment at 10 and 50 μM for 12 h increased mRNA expression of Bax in a concentration-dependent manner ($p < 0.05$ or 0.01, Fig.4B). After TCS treatment with10 and 50 μM for 12 h, Bax protein levels were increased ($p < 0.01$, Fig.4D). There were no significant effects of TCS treatment on Bcl-2 ($p > 0.05$, Fig.4A and C).

3.5. TCS treatment inhibited AKT/mTOR and activated the p38 pathway in PC12 cells

After treatment with 10 and 50 μM TCS for 12 h, phosphorylation of Akt and mTOR was significantly down-regulated ($p < 0.05$ or 0.01, Fig.5A and C). However, there was no effect of TCS on the phosphorylation of AMPK ($p > 0.05$, Fig.5B). Compared with controls, phosphorylation of p38 upon 50 μM TCS treatment was significantly increased in PC12 cells ($p < 0.01$, Fig.5D).

4. Discussion

We report, for the first time, the adverse effects of TCS in PC12 cells. The results of the present study showed that treatment with low levels of TCS (0.05–1 μM) for 48 h caused cell injury, decreasing both the cell viability and increasing LDH release. Moreover, TCS-treated PC12 cells showed activation of Bax protein expression. Additionally, TCS exposure induced an increase in ROS generation accompanied by the inhibition of Akt/mTOR and activation of p38 pathway.

Apoptosis is a physiology or pathology-dependent death process of cells which is caused through a regulated sequence of events and regulated by various pathways. It is also an important indicator to assess the potential cytotoxicity of exogenous chemicals. A large number of studies have shown that TCS activates apoptotic pathway in numerous cell types in different species, including embryonic murine stem cells (Chen et al., 2015), lung epithelial cells(Kwon et al., 2013), clam hemocytes (Matozzo et al., 2012), mice hepatocytes (Yueh et al., 2014), human gingival cells (Zuckerbraun et al., 1998) and human JEG-3 choriocarcinoma cells (Honkisz et al., 2012). TCS also has been found to have apoptotic effects on neuronal cells. For example, an earlier study has shown that long-term exposure to TCS at non-cytotoxic levels induced activation of the extrinsic apoptotic pathways, FasR and caspase-8, as well as secondary necrosis resulting in LDH release in primary cultured cortical neurons. Subsequently, Szychowski et al (Szychowski et al., 2015, 2016) reported that TCS (10 μM) had a cytotoxic effect on the CNS by stimulating caspase-3 activity and resulting in LDH release in neocortical neurons. However, a lower level of TCS treatment (50 nM) for a longer time period (24 h) was sufficient to activate this caspase. Subsequently, it was shown that TCS induced a significant decrease in cell viability in rat neural stem cells (NSC) in a concentration-dependent manner, concomitant with suppressed expression of the anti-apoptotic gene Bcl-2, as well as increased expression of cleaved caspase-3 and the pro-apoptotic gene Bax (Park et al., 2016). The present study demonstrated that 0.001–100 μM TCS treatment for a short period (3 or 6 h) had not significant effects on cell viability in PC12. At lower dose (10 μM) of TCS treatment for a longer exposure period (24 h) decreased cell viability accompanied by increased levels of LDH release. Additionally, 10 and 50 μM TCS treatment for 12 h increased mRNA and protein expression of Bax, absent an effect on Bcl-2 expression. These results indicated that TCS leads to PC12 cells injury by inducing pro-apoptosis and necrosis, establishing putative mechanisms for its neurotoxicity.

ROS are single-electron reduction products of oxygen gas in the body. They contain superoxide anion radicals, peroxide, hydroxyl radicals and nitric oxide etc. Due to the critical role of ROS and its derivatives in apoptosis and necrosis induced by internal metabolism or exogenous chemicals, the occurrences of many diseases have been confirmed to relate with it (Singh et al., 2019; Villamor et al., 2019). Numerous studies have reported that ROS is involved in TCS-induced cellular injury in various living organisms (Zhang et al., 2018; Dubey et al., 2019; Parenti et al., 2019). To date, ROS also has been considered as the primary mechanism of TCS-induced neurotoxicity. For instance, Szychowski et al (Szychowski et al., 2015) found that there is a closely relationship between the pro-apoptotic effects on primary cultured mice neocortical neurons and the increase of ROS induced by TCS. Furthermore, the NSC study suggested that TCS affected ROS homeostasis by decreasing cellular glutathione concentrations and causing oxidative stress and apoptosis (Park et al., 2016). In addition, previous studies reported that mRNA expressions of the main antioxidant enzymes (including catalase, glutathione peroxidase -3 and superoxide dismutase-2) were decreased upon TCS-treatment in rat hypothalamus leading to uncontrolled ROS generation (Wang et al., 2018a,b,c). The present study demonstrated that treatment with 1 and 10 μM TCS for various time points increased the generation of ROS in PC12 cells. Pretreatment with NAC (a ROS scavenger) for 1 h normalized the ROS generation in TCS-treated PC12 cells which consistent with earlier studies (Szychowski et al., 2016). The above-mentioned evidence corroborates the involvement of oxidative stress in neurons upon TCS treatment.

Akt, also known as protein kinase B, plays a key role in the regulations of various cellular processes including cell apoptosis (Chen et al., 2019; Yang et al., 2019). The activation of Akt/mTOR, however, may result in maintenance of cell survival by inhibiting cell apoptosis. An earlier study has demonstrated that exposure to TCS at environmentally relevant concentrations increased mRNA and protein expression of total-AMPK, as well as its activity in mussels (Goodchild et al., 2016). Furthermore, both *in vitro* and *in vivo* studies showed that TCS stimulated autophagy in non-phagocytic cells in a concentration-dependent manner by activating the AMPK/ULK1 and MAPK pathways, independent of the mTOR pathway (Wang et al., 2018a,b,c). Gao et al (Cao et al., 2017) have shown that TCS inhibited the Akt-mTOR signaling pathway, decreasing fetal body weight. Additionally, various studies have reported that the Akt/AMPK-mTOR signaling pathways play an important role in mediating apoptosis, degeneration and necrosis induced by environmental contaminations, and aberrant activations of these pathways has been shown in various neurotoxic injuries and neurodegenerative diseases (Peres et al., 2018; Dinda et al., 2019; Muraleva et al., 2019; Rai et al., 2019). Multiple signal pathways have been shown to be related to the adverse effects of TCS in CNS, including

Fas-dependent apoptosis, NMDAR-dependent ROS generation and necrosis, hippocampal Ca2+, AhR and Cyp1a1/Cyp1b1 pathways and caspase-3-dependent apoptosis etc (Szychowski et al., 2016; Arias-Cavieres et al., 2018; Szychowski et al., 2019). However, whether the Akt/AMPK-mTOR signal pathways are involved in TCS-induced neurotoxicity has yet to be established. The present study demonstrated that treatment with 10 and 50 μM TCS suppressed the Akt/mTOR pathway by inhibiting the phosphorylation of Akt and mTOR in PC12 cells, but not the AMPK pathway, suggesting the potential roles of Akt/AMPK-mTOR signaling pathways in the mechanisms of TCS-induced neurotoxicity.

An *in vivo* study reported that the activations of JNK and p38 MAPK pathways in Sprague Dawley(SD) rat hypothalamus in a concentrations-dependent manner after exposed to 75 ˜300 mg/kg/day TCS via gavage (Axelstad et al., 2013). Further, *in vitro* studies also have demonstrated that phosphorylation of p38 or JNK were involved in TCS-induced apoptosis in human thyroid follicular epithelial cell line Nthy-ori 3-1 cells, but not the MAPK/ERK pathway (Zhang et al., 2018). Co-treatment with NAC and TCS suppressed the phosphorylation of p38, suggesting that oxidative stress closely correlated with TCS-induced activation of the p38 MAPK pathway. Additionally, other investigator showed that TCS treatment activated the phosphorylation of PI3K, ERK and Akt in JB6 Cl 41-5a cells in a concentration-dependent manner, but absent significant effects on the p38 MAPK pathway (Wu et al., 2015). In embryonic stem cells, low levels of TCS treatment specifically induced activation of the ERK MAPK pathway, rather than JNK or p38 MAPK pathway (Cheng et al., 2019). In contrast, Park et al(Park et al., 2016) reported that TCS treatment activated the phosphorylations of JNK and p38 in cultured rat NSCs, but decreased the phosphorylations of ERK, PI3K and Akt. Taken together, the above-mentioned studies indicate that p38 pathway may play a critical role in TCS-induced ROS generation. Thus, the present study focused only on changes in p38 levels rather than other MAPKs. The results showed that TCS at the highest concentration (50 μM for 12 h) activated the p38 phosphorylation. Our main findings are summarized in Fig.6. The reasons for these somewhat contradictory results may be due to the different cell types, different doses and exposure periods of TCS that were used.

5. Conclusion

The current study demonstrated that at a certain concentration range TCS may cause PC12 cells injury via decreasing their cell viability and inducing cell membrane damages. Furthermore, the present study shows that TCS increase the mRNA and protein expressions of apoptosis-related gene Bax without alterations in Bcl-2. Additionally, the results indicate that the Akt/mTOR and p38 pathways, but not AMPK pathway, play a role in TCS-induced uncontrolled ROS generations. Given our finding, and the above mentioned inconsistencies in the effects of TCS in various cell types, future studies on TCS neurotoxicity could be profitably designed to further evaluate the mechanisms by which TCS affects the function of the nervous system, focusing on primary neurons, and/or *in vivo* studies.

Declaration of Competing Interest

The authors declare no conflict of interest.

Acknowledgments

Michael Aschner was partially supported by grants from the National Institute of Environmental Health Sciences (NIEHS R01ES07331, NIEHS R01ES10563 and NIEHS R01ES020852).

References

Allmyr, M., Adolfsson-Erici, M., McLachlan, M.S., Sandborgh-Englund, G., 2006. Triclosan in plasma and milk from Swedish nursing mothers and their exposure via personal care products. Sci. Total Environ. 372 (1), 87–93.

Allmyr, M., Harden, F., Toms, L.M., Mueller, J.F., McLachlan, M.S., Adolfsson-Erici, M., Sandborgh-Englund, G., 2008. The influence of age and gender on triclosan concentrations in Australian human blood serum. Sci. Total Environ. 393 (1), 162–167.

Arias-Cavieres, A., More, J., Vicente, J.M., Adasme, T., Hidalgo, J., Valdes, J.L., Humeres, A., Valdes-Undurraga, I., Sanchez, G., Hidalgo, C., Barrientos, G., 2018. Triclosan impairs hippocampal synaptic plasticity and spatial memory in male rats. Front. Mol. Neurosci. 11, 429.

Axelstad, M., Boberg, J., Vinggaard, A.M., Christiansen, S., Hass, U., 2013. Triclosan exposure reduces thyroxine levels in pregnant and lactating rat dams and in directly exposed offspring. Food Chem. Toxicol. 59, 534–540.

Bagley, D.M., Lin, Y.J., 2000. Clinical evidence for the lack of triclosan accumulation from daily use in dentifrices. Am. J. Dent. 13 (3), 148–152.

Bedoux, G., Roig, B., Thomas, O., Dupont, V., Le Bot, B., 2012. Occurrence and toxicity of antimicrobial triclosan and by-products in the environment. Environ. Sci. Pollut. Res. Int. 19 (4), 1044–1065.

Benseny-Cases, N., Alvarez-Marimon, E., Castillo-Michel, H., Cotte, M., Falcon, C., Cladera, J., 2018. Synchrotron-Based Fourier Transform Infrared Microspectroscopy (muFTIR) Study on the Effect of Alzheimer's Abeta Amorphous and Fibrillar Aggregates on PC12 Cells. Anal. Chem. 90 (4), 2772–2779.

Cao, X., Hua, X., Wang, X., Chen, L., 2017. Exposure of pregnant mice to triclosan impairs placental development and nutrient transport. Sci. Rep. 7, 44803.

Chen, S., Zhuang, K., Sun, K., Yang, Q., Ran, X., Xu, X., Mu, C., Zheng, B., Lu, Y., Zeng, J., Dai, Y., Sushmita, P., Ran, Y., 2019. Itraconazole induces regression of infantile hemangioma via down-regulation of the PDGF-D/PI3K/Akt/mTOR pathway. J. Invest. Dermatol. 106 (2 Pt 1), 628–636.

Chen, X., Xu, B., Han, X., Mao, Z., Chen, M., Du, G., Talbot, P., Wang, X., Xia, Y., 2015. The effects of triclosan on pluripotency factors and development of mouse embryonic stem cells and zebrafish. Arch. Toxicol. 89 (4), 635–646.

Cheng, W., Yang, S., Liang, F., Wang, W., Zhou, R., Li, Y., Feng, Y., Wang, Y., 2019. Low-dose exposure to triclosan disrupted osteogenic differentiation of mouse embryonic stem cells via BMP/ERK/Smad/Runx-2 signalling pathway. Food Chem. Toxicol. 127, 1–10.

Cherednichenko, G., Zhang, R., Bannister, R.A., Timofeyev, V., Li, N., Fritsch, E.B., Feng, W., Barrientos, G.C., Schebb, N.H., Hammock, B.D., Beam, K.G., Chiamvimonvat, N., Pessah, I.N., 2012. Triclosan impairs excitation-contraction coupling and Ca2+ dynamics in striated muscle. Proc Natl Acad Sci U S A 109 (35), 14158–14163.

Dayan, A.D., 2007. Risk assessment of triclosan [Irgasan] in human breast milk. Food Chem. Toxicol. 45 (1), 125–129.

Dinda, B., Dinda, M., Kulsi, G., Chakraborty, A., Dinda, S., 2019. Therapeutic potentials of plant iridoids in Alzheimer's and Parkinson's diseases: a review. Eur. J. Med. Chem. 169, 185–199.

Dirtu, A.C., Roosens, L., Geens, T., Gheorghe, A., Neels, H., Covaci, A., 2008. Simultaneous determination of bisphenol A, triclosan, and tetrabromobisphenol A in human serum using solid-phase extraction and gas chromatography-electron capture negative-ionization mass spectrometry. Anal. Bioanal. Chem. 391 (4), 1175–1181.

Dix-Cooper, L., Kosatsky, T., 2019. Use of antibacterial toothpaste is associated with higher urinary triclosan concentrations in Asian immigrant women living in Vancouver. Canada. Sci Total Environ 671, 897–904.

Dubey, D., Srivastav, A.K., Singh, J., Chopra, D., Qureshi, S., Kushwaha, H.N., Singh, N., Ray, R.S., 2019. Photoexcited triclosan induced DNA damage and oxidative stress via p38 MAP kinase signaling involving type I radicals under sunlight/UVB exposure. Ecotoxicol. Environ. Saf. 174, 270–282.

Geens, T., Neels, H., Covaci, A., 2012. Distribution of bisphenol-A, triclosan and n-nonylphenol in human adipose tissue, liver and brain. Chemosphere 87 (7), 796–802.

Goodchild, C.G., Frederich, M., Zeeman, S.I., 2016. Is altered behavior linked to cellular energy regulation in a freshwater mussel (Elliptio complanata) exposed to triclosan? Comp. Biochem. Physiol. C Toxicol. Pharmacol. 179, 150–157.

Greene, L.A., Tischler, A.S., 1976. Establishment of a noradrenergic clonal line of rat adrenal pheochromocytoma cells which respond to nerve growth factor. Proc. Natl. Acad. Sci. U. S. A 73 (7), 2424–2428.

Heidler, J., Halden, R.U., 2007. Mass balance assessment of triclosan removal during conventional sewage treatment. Chemosphere 66 (2), 362–369.

Honkisz, E., Zieba-Przybylska, D., Wojtowicz, A.K., 2012. The effect of triclosan on hormone secretion and viability of human choriocarcinoma JEG-3 cells. Reprod. Toxicol. 34 (3), 385–392.

Jackson-Browne, M.S., Papandonatos, G.D., Chen, A., Calafat, A.M., Yolton, K., Lanphear, B.P., Braun, J.M., 2018. Identifying vulnerable periods of neurotoxicity to triclosan exposure in children. Environ. Health Perspect. 126 (5), 057001.

Juric, A., Singh, K., Hu, X.F., Chan, H.M., 2019. Exposure to triclosan among the Canadian population: results of the Canadian Health Measures Survey (2009-2013). Environ. Int. 123, 29–38.

Kalloo, G., Calafat, A.M., Chen, A., Yolton, K., Lanphear, B.P., Braun, J.M., 2018. Early life Triclosan exposure and child adiposity at 8 Years of age: a prospective cohort study. Environ. Health 17 (1), 24.

Koeppe, E.S., Ferguson, K.K., Colacino, J.A., Meeker, J.D., 2013. Relationship between urinary triclosan and paraben concentrations and serum thyroid measures in NHANES 2007-2008. Sci. Total Environ. 445-446, 299–305.

Kwon, J.T., Yang, Y.S., Kang, M.S., Seo, G.B., Lee, D.H., Yang, M.J., Shim, I., Kim, H.M., Kim, P., Choi, K., Lee, K., 2013. Pulmonary toxicity screening of triclosan in rats after intratracheal instillation. J. Toxicol. Sci. 38 (3), 471–475.

Liu, J., Wang, J., Zhao, C., Hay, A.G., Xie, H., Zhan, J., 2016. Triclosan removal in wetlands constructed with different aquatic plants. Appl. Microbiol. Biotechnol. 100 (3), 1459–1467.

Matozzo, V., Costa Devoti, A., Marin, M.G., 2012. Immunotoxic effects of triclosan in the

clam Ruditapes philippinarum. Ecotoxicology 21 (1), 66–74.
Muraleva, N.A., Kolosova, N.G., Stefanova, N.A., 2019. p38 MAPK-dependent alphaB-crystallin phosphorylation in Alzheimer's disease-like pathology in OXYS rats. Exp. Gerontol. 119, 45–52.
Mustafa, M., Wondimu, B., Hultenby, K., Yucel-Lindberg, T., Modeer, T., 2003. Uptake, distribution and release of 14C-triclosan in human gingival fibroblasts. J. Pharm. Sci. 92 (8), 1648–1653.
Parenti, C.C., Ghilardi, A., Della Torre, C., Mandelli, M., Magni, S., Del Giacco, L., Binelli, A., 2019. Environmental concentrations of triclosan activate cellular defence mechanism and generate cytotoxicity on zebrafish (Danio rerio) embryos. Sci. Total Environ. 650 (Pt 2), 1752–1758.
Park, B.K., Gonzales, E.L., Yang, S.M., Bang, M., Choi, C.S., Shin, C.Y., 2016. Effects of triclosan on neural stem cell viability and survival. Biomol. Ther. (Seoul) 24 (1), 99–107.
Peres, T.V., Arantes, L.P., Miah, M.R., Bornhorst, J., Schwerdtle, T., Bowman, A.B., Leal, R.B., Aschner, M., 2018. Role of Caenorhabditis elegans AKT-1/2 and SGK-1 in manganese toxicity. Neurotox. Res. 34 (3), 584–596.
Pycke, B.F., Geer, L.A., Dalloul, M., Abulafia, O., Jenck, A.M., Halden, R.U., 2014. Human fetal exposure to triclosan and triclocarban in an urban population from Brooklyn, New York. Environ. Sci. Technol. 48 (15), 8831–8838.
Rai, S.N., Dilnashin, H., Birla, H., Singh, S.S., Zahra, W., Rathore, A.S., Singh, B.K., Singh, S.P., 2019. The role of PI3K/Akt and ERK in neurodegenerative disorders. Neurotox. Res. 35 (3), 775–795.
Rodricks, J.V., Swenberg, J.A., Borzelleca, J.F., Maronpot, R.R., Shipp, A.M., 2010. Triclosan: a critical review of the experimental data and development of margins of safety for consumer products. Crit. Rev. Toxicol. 40 (5), 422–484.
SCCS, 2010. Opinion on Triclosan (antimicrobial Resistance) European Commission.
Singer, H., Muller, S., Tixier, C., Pillonel, L., 2002. Triclosan: occurrence and fate of a widely used biocide in the aquatic environment: field measurements in wastewater treatment plants, surface waters, and lake sediments. Environ. Sci. Technol. 36 (23), 4998–5004.
Singh, A., Kukreti, R., Saso, L., Kukreti, S., 2019. Oxidative stress: a key modulator in neurodegenerative diseases. Molecules 24 (8).
Szychowski, K.A., Sitarz, A.M., Wojtowicz, A.K., 2015. Triclosan induces Fas receptor-dependent apoptosis in mouse neocortical neurons in vitro. Neuroscience 284, 192–201.
Szychowski, K.A., Wnuk, A., Kajta, M., Wojtowicz, A.K., 2016. Triclosan activates aryl hydrocarbon receptor (AhR)-dependent apoptosis and affects Cyp1a1 and Cyp1b1 expression in mouse neocortical neurons. Environ. Res. 151, 106–114.
Szychowski, K.A., Wnuk, A., Rzemieniec, J., Kajta, M., Leszczynska, T., Wojtowicz, A.K., 2019. Triclosan-evoked neurotoxicity involves NMDAR subunits with the specific role of GluN2A in Caspase-3-Dependent apoptosis. Mol. Neurobiol. 56 (1), 1–12.
Tanoue, R., Nomiyama, K., Nakamura, H., Hayashi, T., Kim, J.W., Isobe, T., Shinohara, R., Tanabe, S., 2014. Simultaneous determination of polar pharmaceuticals and personal care products in biological organs and tissues. J. Chromatogr. A 1355, 193–205.
Villamor, E., Moreno, L., Mohammed, R., Perez-Vizcaino, F., Cogolludo, A., 2019. Reactive oxygen species as mediators of oxygen signaling during fetal-to-neonatal circulatory transition. Free Radic. Biol. Med.
Wang, C., Chen, L., Zhao, S., Hu, Y., Zhou, Y., Gao, Y., Wang, W., Zhang, J., Tian, Y., 2018a. Impacts of prenatal triclosan exposure on fetal reproductive hormones and its potential mechanism. Environ. Int. 111, 279–286.
Wang, C., Yu, Z., Shi, X., Tang, X., Wang, Y., Wang, X., An, Y., Li, S., Li, Y., Wang, X., Luan, W., Chen, Z., Liu, M., Yu, L., 2018b. Triclosan enhances the clearing of pathogenic intracellular Salmonella or Candida albicans but disturbs the intestinal microbiota through mTOR-Independent autophagy. Front. Cell. Infect. Microbiol. 8, 49.
Wang, F., Liu, F., Chen, W., Xu, R., Wang, W., 2018c. Effects of triclosan (TCS) on hormonal balance and genes of hypothalamus-pituitary- gonad axis of juvenile male Yellow River carp (Cyprinus carpio). Chemosphere 193, 695–701.
Wang, L., Asimakopoulos, A.G., Kannan, K., 2015. Accumulation of 19 environmental phenolic and xenobiotic heterocyclic aromatic compounds in human adipose tissue. Environ. Int. 78, 45–50.
Wu, Y., Beland, F.A., Chen, S., Fang, J.L., 2015. Extracellular signal-regulated kinases 1/2 and Akt contribute to triclosan-stimulated proliferation of JB6 Cl 41-5a cells. Arch. Toxicol. 89 (8), 1297–1311.
Yan, Z.R., Meng, H.S., Yang, X.Y., Zhu, Y.Y., Li, X.Y., Xu, J., Sheng, G.P., 2019. Insights into the interactions between triclosan (TCS) and extracellular polymeric substance (EPS) of activated sludge. J. Environ. Manage. 232, 219–225.
Yang, X., Zhao, T., Feng, L., Shi, Y., Jiang, J., Liang, S., Sun, B., Xu, Q., Duan, J., Sun, Z., 2019. PM2.5-induced ADRB2 hypermethylation contributed to cardiac dysfunction through cardiomyocytes apoptosis via PI3K/Akt pathway. Environ. Int. 127, 601–614.
Yu, L., Ling, G., Deng, X., Jin, J., Jin, Q., Guo, N., 2011. In vitro interaction between fluconazole and triclosan against clinical isolates of fluconazole-resistant Candida albicans determined by different methods. Antimicrob. Agents Chemother. 55 (7), 3609–3612.
Yueh, M.F., Taniguchi, K., Chen, S., Evans, R.M., Hammock, B.D., Karin, M., Tukey, R.H., 2014. The commonly used antimicrobial additive triclosan is a liver tumor promoter. Proc Natl Acad Sci U S A 111 (48), 17200–17205.
Zhang, N., Peng, F., Ying, G.G., Van den Brink, P.J., 2019. Fate and effects of triclosan in subtropical river biofilms. Aquat. Toxicol. 212, 11–19.
Zhang, P., Yang, M., Zeng, L., Liu, C., 2018. P38/TRHr-dependent regulation of TPO in thyroid cells contributes to the hypothyroidism of triclosan-treated rats. Cell. Physiol. Biochem. 45 (4), 1303–1315.
Zhao, T., Su, G., Wang, S., Zhang, Q., Zhang, J., Zheng, L., Sun, B., Zhao, M., 2017. Neuroprotective effects of acetylcholinesterase inhibitory peptides from anchovy (Coilia mystus) against glutamate-induced toxicity in PC12 cells. J. Agric. Food Chem. 65 (51), 11192–11201.
Zhou, Z., Yang, J., Chan, K.M., 2017. Toxic effects of triclosan on a zebrafish (Danio rerio) liver cell line. ZFL. Aquat Toxicol 191, 175–188.
Zuckerbraun, H.L., Babich, H., May, R., Sinensky, M.C., 1998. Triclosan: cytotoxicity, mode of action, and induction of apoptosis in human gingival cells in vitro. Eur. J. Oral Sci. 106 (2 Pt 1), 628–636.